One-heater flow-through polymerase chain reaction device by heat pipes cooling

Jyh Jian Chen,[1,a)] Ming Huei Liao,[2] Kun Tze Li,[1] and Chia Ming Shen[1]
[1]*Department of Biomechatronics Engineering, National Pingtung University of Science and Technology, 1, Shuefu Road, Neipu, Pingtung 91201, Taiwan*
[2]*Department of Veterinary Medicine, National Pingtung University of Science and Technology, 1, Shuefu Road, Neipu, Pingtung 91201, Taiwan*

(Received 20 October 2014; accepted 13 January 2015; published online 22 January 2015)

This study describes a novel microfluidic reactor capable of flow-through polymerase chain reactions (PCR). For one-heater PCR devices in previous studies, comprehensive simulations and experiments for the chip geometry and the heater arrangement were usually needed before the fabrication of the device. In order to improve the flexibility of the one-heater PCR device, two heat pipes with one fan are used to create the requisite temperature regions in our device. With the integration of one heater onto the chip, the high temperature required for the denaturation stage can be generated at the chip center. By arranging the heat pipes on the opposite sides of the chip, the low temperature needed for the annealing stage is easy to regulate. Numerical calculations and thermal measurements have shown that the temperature distribution in the five-temperature-region PCR chip would be suitable for DNA amplification. In order to ensure temperature uniformity at specific reaction regions, the Re of the sample flow is less than 1. When the microchannel width increases and then decreases gradually between the denaturation and annealing regions, the extension region located in the enlarged part of the channel can be observed numerically and experimentally. From the simulations, the residence time at the extension region with the enlarged channel is 4.25 times longer than that without an enlarged channel at a flow rate of 2 μl/min. The treated surfaces of the flow-through microchannel are characterized using the water contact angle, while the effects of the hydrophilicity of the treated polydimethylsiloxane (PDMS) microchannels on PCR efficiency are determined using gel electrophoresis. By increasing the hydrophilicity of the channel surface after immersing the PDMS substrates into Tween 20 (20%) or BSA (1 mg/ml) solutions, efficient amplifications of DNA segments were proved to occur in our chip device. To our knowledge, our group is the first to introduce heat pipes into the cooling module that has been designed for a PCR device. The unique architecture utilized in this flow-through PCR device is well applied to a low-cost PCR system.
[http://dx.doi.org/10.1063/1.4906505]

INTRODUCTION

Polymerase chain reaction (PCR) is one of the most common techniques for deoxyribonucleic acid (DNA) amplification outside the body. PCR technology can replicate copies of DNA fragments from small to large samples of reactants for detection. It has been widely used in biological science, clinical medicine, genetic disease diagnostics, food safety testing, and other related fields. PCR typically requires thermocycling to sequentially bring template DNA through the denaturation, annealing, and extension stages at three different temperatures.

[a)]Author to whom correspondence should be addressed. Electronic mail: chaucer@mail.npust.edu.tw. Tel.: +886 8 7703202 ext. 7029; Fax: +886 8 7740420.

During traditional PCR, the large thermal mass of the thermocycler slows down the heat transfer to the sample and the heat dissipation from the sample. So it increases the required time for DNA amplification.

The concept of microfluidic technology has accelerated the miniaturization of analysis instruments in biochemistry. The PCR chip has many advantages, such as portability, shortened thermal cycling time, and reduced reagent consumption. During the last few decades, PCR chips have gained a lot of attention due to their small thermal masses and the large heat transfer rate inside the system. The designs of the PCR chips can be categorized as the chamber type and the flow-through type. Each type has its own merits. The PCR chips integrated with different functions have been investigated in many studies. Liu *et al.* have reported on the recent evolution in the development of PCR microreactors.[1]

Since the PCR process is completed under several dozens of thermal circulations, the flow-through PCR device can regulate the temperature of the reactants based on the movement of the reactants through different temperature regions. By excluding the substrate from the thermal cycling, this device can speed up the transition time, quicken the thermal response, and reduce the reaction time. Most flow-through PCR devices have implemented three heaters to provide three temperature regions. However, heat management without thermal cross-talk is difficult in these devices. The devices require enough space (the width of the chip is usually larger than 30 mm) between the heaters to avoid thermal cross-talk. Furthermore, to realize the required extension times over the narrow zone, additional loops on each extension region are usually integrated. The additional loops may increase the chip size required for PCR.[2]

Controlling the multiple temperature regions in the microfluidic chips is not easy, so reducing the number of heaters inside the PCR system has attracted some researchers' attention. When the entire sample has reached the requisite PCR temperatures, the denaturation and annealing reactions happen almost instantaneously (e.g., they continue for less than 1 s), and the extension rate is on the order of 60–100 bases per second.[3] A previous study showed that the extension stage can occur during the transition between annealing and denaturation temperatures and no hold time is required when the DNA amplification targets are few. It can result in a rapid amplification cycle, no loss in amplification efficiency, low cost, and high specificity.[4] There have been some reports on performing flow-through PCR for two-temperature thermal cycling inside the microdevice.[5–10] Some of them combine the annealing and extension stages at the same temperature region, or the extension region is not created by direct heating but by lateral heat conduction from heaters for denaturation and annealing.

The control of multiple temperatures is one of the limitations of adopting a flow-through type PCR device. Researchers have strived to reduce the number of heaters by utilizing a single heater and creating the appropriate reaction regions for PCR. Crews *et al.* were the first group who utilized a single heater to perform flow-through PCR. They used two microscope slides to fabricate a glass-based PCR chip with the heater in the middle part of the chip, the heat sinks on the opposite sides of the chip, and a serpentine channel with varying widths.[11] Wu and Lee proposed the fabrication of a three-dimensional microdevice employing a single heater. By adjusting the thickness of the substrate, they could use only one heater to control two temperatures of an on-chip PCR.[12] Sciancalepore *et al.* presented a microdroplet-based multiplex PCR device for the detection of bacterial genes. Only one heater was required to obtain the desired PCR thermal profile.[13] Trinh *et al.* fabricated a polymer-glass hybrid microdevice to perform PCR employing a single heater. Invar, as an intermediate layer, was inserted between the device and the heater to create a temperature gradient on a microdevice. By manually varying the protrusion length of the Invar sheet from the heater, the areas for different PCR temperature regions could be altered on the chip.[14]

The geometrical design and the pattern arrangement of the serpentine channel in the flow-through PCR chip ensure the reduction of the total reaction time and the limitation of the overall chip size. The layout of the channel must be consistent with the configurations of the heating assemblies. With a constant width and depth of the microchannel, the length of the extension region is usually greater than that of the denaturation or annealing regions in a PCR chip.[2] This results in the increasing of the transitional time. The transitional time is the time period in which

the sample is traveling between temperature regions. To eliminate the extended time periods, a small width of the microchannel in the transitional regions and a large width in the reaction regions is suggested. This can accelerate the sample through the transitional regions and optimize the reaction time in the reaction regions. Li *et al*. presented a PCR microdevice which contains a serpentine microchannel with varying widths and a constant depth. The varying widths of the channel significantly reduced the transitional periods.[15] Cao *et al*. demonstrated three thermoplastic PCR devices with different channel dimensions which resulted in changes in the residence times. Residence time is defined as the average amount of time that a sample spends in a particular reaction region. The denaturation and annealing regions were designed to be narrower than the extension region.[10]

On conventional layouts with three heating regions, large sized chip modules are required for a suitable arrangement of the microchannel to complete the PCR process. The developed five-temperature-region thermocycler concept overcomes these limitations. Temperature regions are crosswisely arranged (i.e., annealing, extension, denaturation, extension, and annealing regions) to avoid the need for an additional denaturation region. Thus, chip size can be used more efficiently. The five regions design requires only one half-loop per PCR cycle. Hashimoto *et al*. fabricated a chip for the analysis of single base mutations in genomic DNA. Three different Kapton film heaters were attached to the appropriate positions on the chip to provide the required temperature regions. The arrangement of the reaction regions on the microchannel (368 K for denaturing and 333 K for annealing/extension) was depicted.[16] Crews *et al*. manufactured a glass PCR microchip. The edges of their device were cooled simply by air exposure. The appropriate temperature distribution for PCR was generated by one heater held at a steady state temperature.[11] Reichert *et al*. reported on the application of thermal management for PCR using five temperature regions. Each temperature region contained a copper blade equipped with a self-adhesive heating film and a temperature sensor.[17]

Constructing several distinct temperature regions within a small chip is complicated. Implementation of three heaters to provide three temperature regions was commonly utilized in previous studies. However, heat management without thermal cross-talk is difficult by imposing three heaters on the chip. Some researchers have reduced the number of heaters inside the PCR system to one while still obtaining the desired PCR thermal profile. This method is able to considerably decrease the complexity of system integration and the cost of the device, making this PCR system especially attractive for bio-laboratories. A novel one-heater CFPCR microchip was first integrated by the Crews group. For a one-heater PCR device, comprehensive numerical calculations and repetitive experiments for the chip geometry and the heater arrangement are usually needed before the fabrication of the device. Then, the requisite PCR thermal profile can be realized in the chip, and the chip can carry out the PCR experiment successfully. However, when the DNA sample is changed and the required PCR temperatures have to be adjusted occasionally, the chip geometry and the heater arrangement need to be redesigned. Lack of flexibility is one of the main drawbacks in the one-heater PCR device.

In order to improve the flexibility of the one-heater PCR chip, heat pipes with a fan are used in our study to create the other temperature regions of the chip. The heat pipes are thermal superconductors and are very cheap. With the integration of one heater onto the chip center, the high temperature for the denaturation stage can be generated. By arranging the heat pipes on the opposite sides of the chip, the low temperature for the annealing stage is easy to regulate. Thus, the temperature for the extension stage is created amid the denaturation and the annealing regions based on Fourier's law. Therefore, constructing five temperature regions in the related fields of the flow-through PCR system within a small chip is obtained. Furthermore, by the rearrangement and enlargement of the channel width at the extension region, the residence time during the extension stage can be properly extended. This certainly helps in achieving successful DNA amplification.

In this paper, a flow-through PCR device with simple integration and low cost is proposed. To our knowledge, our group is the first group to introduce heat pipes into the cooling module in a PCR device. During design, commercial software is used to perform the heat and mass

transfer analysis and ensure the appropriate thermal management of the chip. The microdevice is fabricated by the conventional soft-lithography method. By utilizing one heater and two heat pipes to create the denaturation region and the annealing regions, the chip volume is greatly reduced and the ease of thermal control is increased. Heat pipes with high thermal conductance and low expenditure are utilized. By arranging the heat pipes on the opposite sides of the chip, the low temperature for the annealing stage is easy to regulate. After assembly, the temperature control system specifications are tested and the device is used to set up the DNA amplification function. Furthermore, in order to reduce the protein adsorption on the channel surface, the polydimethylsiloxane (PDMS) microchannel is modified to be hydrophilic by immersing the PDMS substrates into various solutions. The treated surfaces of the flow-through microchannel are characterized using the water contact angle and the effects of the treatments on PCR efficiency are determined using gel electrophoresis.

THEORETICAL MODEL

The flow-through PCR device is modeled to assess the temperature uniformity at the specific regions which is dominated by the ambient conditions, the locations of the heater and the heat pipes, and the sample flow rates inside the microchannel. The physical problem is designing a microfluidic chip based on a single meandering channel passing repetitively through several temperature regions. The complete chip consists of the reaction PDMS channel chip and a cover chip made of glass. The overall dimensions of the PDMS microchannel chip and the glass bonding chip are 35 mm long $\times$ 25 mm wide $\times$ 1.9 mm high and 76 mm long $\times$ 25 mm wide $\times$ 1.1 mm high, respectively. The denaturation (high temperature) region is heated by the heater and arranged at the chip center with both the extension (middle temperature) and the annealing (low temperature) regions at the two sides. The two annealing regions are cooled by two heat pipes with one fan. The extension regions are generated by the thermal gradients between the denaturation and the annealing regions. The chip absorbs the thermal energy from the heater and the stored heat is transferred through the heat pipes or by ambient air from the other surfaces of the chip. A natural convection condition is assumed except for on the heater and the cooler surfaces.

A rectangular microchannel with a depth of 50 μm is utilized in the simulated model. The width of the microchannel either gradually expands from 150 μm to 540 μm and contracts back to 150 μm for the extension region, or 150 μm for the rest. By the enlargement of the channel width at the extension region, the residence time during the extension stage can be properly extended. We use water as the required sample and the fluid properties are set as the physical and thermodynamic properties of water at 300 K. The sample is injected at the inlet at 300 K. Then, it flows repeatedly through the denaturation (368 K), annealing (328 K), and extension (345 K) regions 30 times. Finally, it flows out of the outlet after passing the final extension region at 345 K.

The governing equations consist of conservation of mass, momentum, and energy equations. The conservation of mass and momentum equations are solved to identify the flow fields of the liquids in the microchannel. The conservation of energy equation is utilized to obtain the thermal fields of the total system. The following assumptions have been adopted to obtain a proper mathematical formulation of this problem.

(1) Fluid flow is Newtonian, incompressible, and laminar.
(2) The thermophysical properties of the chip system, such as the density, specific heat, viscosity, and thermal conductivity are temperature-invariant and uniform through the entire chip system during the PCR process.
(3) There are no internal heat sources.
(4) Both the compression work and viscous dissipation of the fluid are negligible.
(5) Thermal radiation energy transfer between the system and the ambient air is not included.
(6) The thermal contact resistance between the chip and the heater or the coolers is not considered, i.e., perfect contact surfaces are assumed.

In symbolic notation, the steady state equations can be expressed in vector forms as follows:

$$\nabla \cdot \vec{U} = 0, \tag{1}$$

$$\vec{U} \cdot \nabla \vec{U} = \frac{-\nabla p}{\rho} + \nu \nabla^2 \vec{U}, \tag{2}$$

$$\vec{U} \cdot \nabla T_1 = \alpha \nabla^2 T_1, \tag{3}$$

$$\nabla^2 T_2 = 0, \tag{4}$$

where $\vec{U}$ is the fluid velocity vector, ρ is the fluid density, p indicates the pressure, ν is the kinematic viscosity of the fluid. T_1 and T_2 indicate the temperatures of the fluid and the solid substrate, respectively. α is the thermal diffusivity. Equation (3) must be solved together with Eqs. (1) and (2) in order to achieve computational coupling between the velocity field solution and the temperature distribution.

The convection effect inside the microchannel on the temperature distributions within the chip and the residence time at each PCR stage are investigated in this study. The sample passes through three PCR stages repeatedly for 30 cycles to complete the PCR process. Recent work[18] provided strong evidence that severe thermal non-uniformities can arise due to the edge effects associated with the finite-array versus the infinite-array of serpentine channel sections. In order to simplify the simulation and reduce the computational time, the computational domain including only 7 of the thermal cycles is simulated and used to obtain the approximated condition.

Boundary conditions are applied to the inlet and outlet as follows. A fixed flow rate condition at a specific value and isothermal condition of 300 K are set at the channel inlet; the boundary condition at the outlet is a fixed pressure. The non-slip boundary condition is used for the microchannel wall. The boundary conditions for the energy equation are as follows and shown in Fig. 1(a). The temperature regions in the device supported by the heater and the heat pipes supply a uniform temperature input, and the isothermal boundary condition is utilized.

$$T_2 = T_{w,region\,i}, \tag{5}$$

where $T_{w,region\ i}$ is the temperature of the isothermal region i. Two constant temperatures set at the high-temperature (denaturation) and low-temperature (annealing) regions are $T_{w,d}$ and $T_{w,a}$, respectively. The symmetric boundary condition is set at two sides of the domain along the x-direction. The convective boundary condition is used on all the other surfaces

$$-k_c \frac{\partial T_2}{\partial n} = h(T_2 - T_\infty), \tag{6}$$

where k_c is the thermal conductivity of the chip material, n is a normal vector field orthogonal to the outer surface, T_∞ is the ambient air temperature, h is the natural convective heat transfer coefficient between the outer surface and the ambient air. An appropriate expression for h can be obtained from the following empirical relation for the corresponding Nusselt number and Rayleigh number:[19]

$$Nu = \frac{hL_c}{k_{air}} = 1.02Ra^{0.148}, \quad Ra = \frac{g\beta(T_{w,d} - T_\infty)L_c^3}{\alpha_{air}\nu_{air}}, \tag{7}$$

where g is gravity and β is the coefficient of volume expansion. L_c is characteristic length and it can be expressed as

$$L_c = \frac{4WL}{2(W+L)}, \tag{8}$$

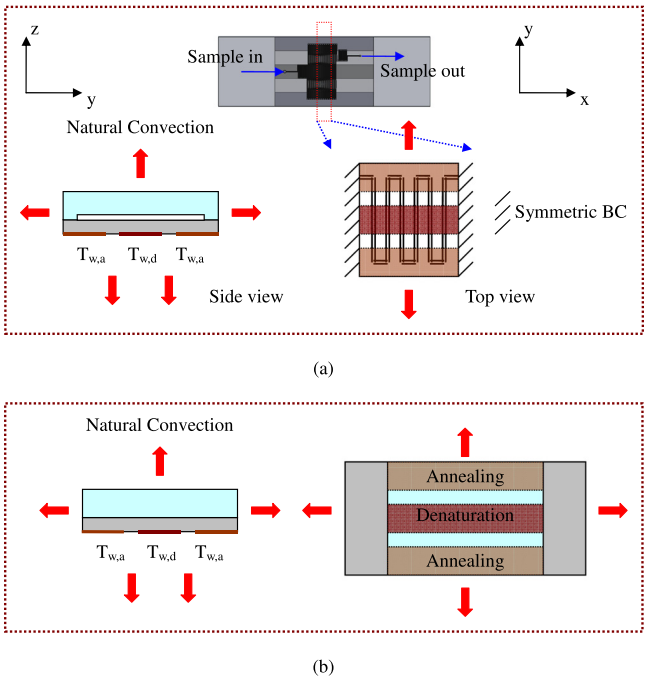

FIG. 1. The boundary conditions for the energy equation (a) with the thermal convection inside the microchannel and the volume of the microchannel and (b) without the thermal convection inside the microchannel and the volume of the microchannel.

where W is the width of the chip and L is the length of the chip. h can be estimated as 5.005 W/m^2 k in our study.

The thermal convection of the sample along the microchannel is one of the most important effects on the volume of the temperature regions for PCR. Above a critical flow rate, the sample fails to achieve the required temperature and/or the requisite residence time for PCR.[7] In order to complete the PCR process without uncertainty, the sample flow rate was chosen to be lower than the critical value. Then, the thermal convection effect along the microchannel on the chip temperature is negligible and the temperature of the sample flow is almost equal to that near the solid wall of the chip. The PCR residence time at each stage can also be estimated. To evaluate the temperature distribution across the total chip system, the thermal convection inside the microchannel and the volume of the microchannel are not included in case the sample flow rate is small. For the solid layer of the chip, i.e., PDMS and glass plates, only Eq. (4) has to be solved and the fluid velocity vector is set to be 0. The boundary conditions for the energy equation are revealed in Fig. 1(b). The natural convection from the ambient air and the thermal conduction inside the chip system are considered. The isothermal boundary conditions, Eq. (5), are utilized. Finally, the convective boundary condition, Eq. (6), is used on all the surfaces except for the isothermal areas.

The computational fluid dynamics package, CFD-ACE+^{TM} (V2006, CFD Research Corporation, Huntsville, AL, USA), which uses a finite volume approach, is utilized to solve the three-dimensional flow and thermal fields and to improve the chip design. A nonlinear steady-state algorithm is used for hydrodynamic calculations, and a linear steady state algorithm is applied to solve the heat transfer equation. Three-dimensional structured grids are used, and the SIMPLEC method is employed for pressure-velocity coupling.[20] The spatial discretizations for the convection terms are performed using a second-order upwind scheme with limiter[21] and the spatial discretizations for the diffusion-like terms are then presented applying a second-order central difference scheme. The simulation is implemented for a steady state. The algebraic multigrid (AMG) solver is utilized for pressure corrections,[22] and the conjugate gradient

squared (CGS) and preconditioning (Pre) solvers are used for velocity and temperature corrections during iteration.[23] The inertial relaxation for velocities is set to 0.1, and the linear relaxation for pressure is set to 0.5. The solution is considered converged when the relative errors of all transported variables are less than 10^{-5} between successive sweeps. In order to achieve grid independence of the numerical results, several grid numbers are investigated by comparing thermal and flow fields at various steps and the grid number is optimized for the accuracy and the speed of the simulation.

MATERIALS AND METHODS

The microfluidic device is composed of a PDMS-based chip, a home-made syringe pump, one heating and one cooling module, and two temperature controllers. A serpentine channel with various widths meandering inside the chip is used for the DNA mixture to be pumped through. The denaturation region supported by one heater is located at the center of the chip and the annealing regions cooled by using two heat pipes are set at the two sides of the chip. The symmetric management creates the five reaction regions in the chip. Two temperature controllers maintain the temperatures of the heating and cooling modules at specific values. A temperature distribution is created along the chip so that the DNA mixture can be heated and cooled during several thermal cycles to finish the PCR process.

Device design

The PCR chip consists of a PDMS and a glass layer with thicknesses of 1.9 and 1.1 mm, respectively, as shown in Fig. 2. The detailed fabrication process of the PDMS-glass bonding chip has been described in the previous work.[2] Two holes working as the inlet and outlet for the PCR mixture are drilled in the PDMS layer. As can be seen from the top view of the schematic drawing of the PCR chip, the total length of the microchannel is 747.79 mm. The 30-loop meandering channel is 50 μm in depth and 150 μm in width except for the extension region, which has a maximum width of 540 μm. The SEM pictures of the microchannels are also shown. The five-temperature-region design requires only one half-loop per PCR cycle in contrast to the conventional three-region design. Through this channel, the sample flows through the denaturation, annealing, and extension regions successively.

Temperature control system

The arrangement of five reaction regions on the chip is carried out in our system. When performing PCR, the PCR chip is attached tightly to the top-side of the heater block and the

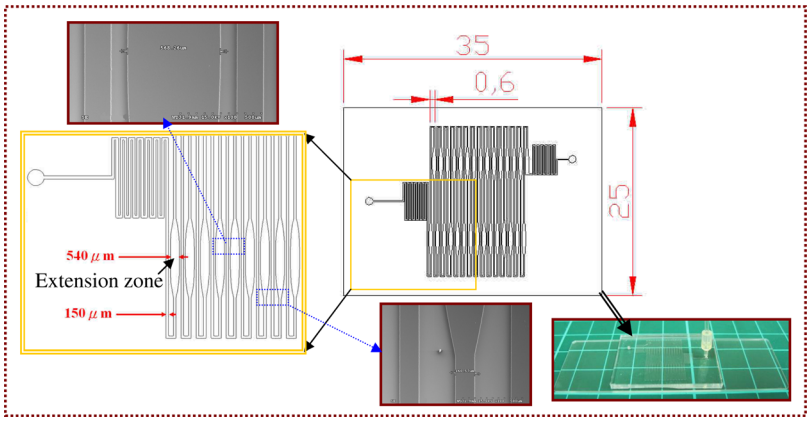

FIG. 2. The PCR chip consists of a PDMS and a glass layer. The top view of the schematic drawing of the PCR chip, the pictures of SEM of microchannel, and the glass-PDMS bonded chip are shown.

cooling module. The aluminum heating block, two heat pipes with a fan, and the PDMS-based chip are assembled and fixed onto a poly(methyl methacrylate) (PMMA) housing. The chip temperature at the denaturation region during the operation is held by using the cartridge heater under a home-made proportional-integral-derivative (PID) controller. The temperature sensor, DS1821 (Dallas Semiconductor, USA), mounted onto the heater is utilized to supply temperature feedback. The annealing temperature is controlled by the contacted heat pipe and the sensor through a similar PID controller.

A thermal control system is utilized to control the power input into the heating and cooling modules and create a stable temperature distribution within the chip. The diagram and the photograph of the control system are shown in Fig. 3. The temperature control system is composed of an AT89S51 microprocessor, an amplifier, a D/C converter, a seven-segment display, a key-press input, an interface with serial port (RS 232), and a power output. The temperature reading as sensed by DS1821 is passed along to the microprocessor. The temperature is displayed on the seven-segment display or recorded in the computer through the interface with port RS 232. The measured temperature is compared with the setting temperature input by the key-presses. The control signal based on the PID scheme determines the power output. Due to the spatial separation, the sensor temperature differs from the temperature of the PCR mixture in the microchannel. Therefore, the microchannel temperature is measured by using thermocouples inserted into the microchannel before the PCR experiment. The measured temperature is utilized to calibrate the sensor temperature to set the feedback control.

An aluminum block, measuring 35 mm long × 6 mm wide × 6 mm high, is integrated onto the chip and utilized at the heating stage.[2] Two 6 mm-diameter heat pipes are pressed flat and contact the chip via some thermal conductive adhesive. A heat pipe can be considered a thermal superconductor that combines the principles of both thermal conduction and phase transition to efficiently manage the transfer of heat between two solid interfaces. The cost for one heat pipe in our system is very cheap; less than $2 USD. The heat pipe allows uniform temperature distribution on the surface and can also be thermally controlled by a fan without difficulty. Attaching a fan to a portion of the heat pipe makes the heat pipe cool to the setting temperature. Accurate temperature control is also achieved using a PID control program.

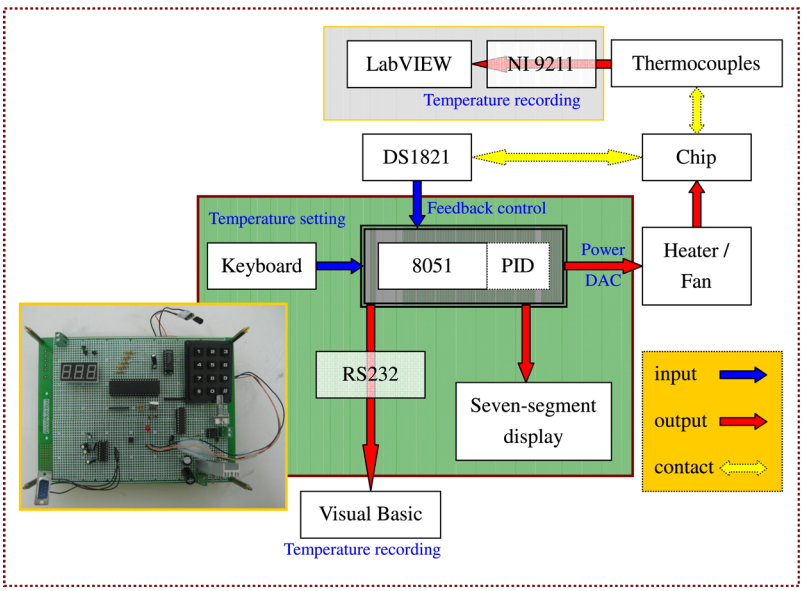

FIG. 3. The structural drawing and the photograph of temperature-controlled system.

Temperature measurement

Temperature uniformity is one of the important issues which influence the efficiency of biological reactions. An infrared (IR) camera (TVS-100, AVIO, Japan) is utilized to characterize the spatial temperature distribution across the surface of the PDMS-based chip and evaluate the performance of the heating and cooling modules. After reaching a steady state temperature distribution, IR images of the PCR device are captured. The captured digital images are then converted into temperature profiles.

The channel temperatures are measured using thermocouples which are injected into the microchannel during bonding and connected to a data acquisition system (Model NI 9211, National Instruments, USA) that converts the analog signal to a digital one. A computer receives the temperature signals through the NI 9211 interface and records the real-time temperature profiles.

The sample transport along the microchannel with various temperature gradients can also be visualized qualitatively using a thermally sensitive dye (TM-SL 70-3441, New Prismatic Enterprise Co., Ltd., Taiwan). Using the thermally sensitive dye with an approximate transition temperature of 343 K, a visualization of the channel temperature distribution can be achieved. The dye becomes colorless when the temperature is greater than approximately 343 K and darker when the temperature is lower than roughly 343 K.

Surface modification and bubble reduction

Due to the high surface-to-volume ratio, a serpentine channel design increases the possibility of proteins (e.g., polymerase) in PCR mixtures sticking onto the hydrophobic surface (contact angle is larger than 90°) of the PDMS microchannel walls. Any polymerase adsorbed by the walls of the chip reduces the PCR efficiency. To reduce polymerase adsorption and PCR inhibition, the microchannel walls are coated with polysorbate 20 (Tween 20) or bovine serum albumin (BSA) to prevent the unspecific binding of DNA polymerase onto them. The treatment involves pre-treating the surface of the material with a substance that is compatible with a PCR reaction and is a static surface modification.[24]

The generation of air bubbles before the introduction of the sample solution into the high-temperature conditions is one of the crucial topics in microfluidic systems. A moderate amount of a highly viscous liquid with a high boiling point (e.g., mineral oil) flows into the microchannel just before the introduction of the sample solution, which helps increase the pressure of the sample solution in the microchannel.[2,9,11,25] Then, the latter solution follows the flowing mineral oil into the high-temperature region without the generation of air bubbles.

PCR chemistry

Q fever, caused by the bacterium *Coxiella burnetii*, has become an emerging public health problem in the world. On the chip and commercial PCR machine, a 385-bp segment of *Coxiella burnetii* DNA is amplified to evaluate the performance of the DNA amplification. The PCR mixture consists of 2 × reaction buffer, 200 μM of each dNTP, 1.5 mM of $MgCl_2$, 0.5 μM of each of the forward and reverse primers, 0.5 U/μl of DNA polymerase, and 0.2 ng/μl of template DNA.

The thermal cycling program for the commercial PCR machine involves heating the mixture at 94 °C for 3 min to activate the polymerase and denature the initial DNA, followed by thermal conditions consisting of denaturing at 94 °C, annealing at 55 °C, and extension at 72 °C for 30 s. Upon completion of up to 30 thermal cycles, the chip is kept at 72 °C for 3 min for final extension. The negative control experiment is conducted by replacing the template genomic DNA with nuclease-free water.

Chip operation

We design a PDMS-based PCR chip consisting of microchannels to perform the PCR process for 30 cycles. On the PDMS substrate, there is a sample loading inlet/outlet port. The chip is placed on the chip holder with one heater and two heat pipes. The heat pipes are in contact with a single fan, which provides cool air to regulate the temperatures of the heat pipes. The static passivation process is carried out before the PCR mixture is loaded into a syringe. The PCR solution introduced into the microchannel by a home-made syringe pump has a specific flow rate. Mineral oil used to suppress the bubble formation in the microchannel is first injected into the microchannel and then followed by the PCR solution.

A syringe pump is useful in microfluidic applications for slow incorporation of a fixed volume of fluid into a microchannel. It is a combination of mechanical and electronic components that manipulate a standard syringe. In our work, a home-made syringe pump costs less than $400 USD and is used to pump the DNA mixture into the chip. A microprocessor controls a continually running motor which applies a continuous force upon the plunger end of the syringe. Our syringe pump features a software interface where a user can control the device to change the flow rate of the fluid. The flow rates for the liquid volumes of 25, 50, and 75 μl at 1 μl/min (theoretical value) are measured, and the average values after 10 measurements are 0.996, 1.028, and 1.036 μl/min, respectively. The maximum relative error is less than 3.6%.

The results are compared with those utilizing the commercial PCR machine. The PCR products are collected in a vial from the channel outlet and mixed with 1 $\times$ blue dye. 10 μl of each sample are loaded onto 2% agarose gel (Certified Molecular Biology Agarose, Bio-Rad, USA) and electrophoresed (Mini-Sub Cell GT System, Bio-Rad, USA) in 10$\times$ Tris/Boric Acid/EDTA (TBE) buffer. The slab gel electrophoresis is run at 350 V for 1 h. After electrophoresis, the gel is stained with 10 mg/ml ethidium bromide solution (Bio-Rad, USA) and visualized by UV transillumination.

RESULTS AND DISCUSSION

In this section, the design concept of the flow-through PCR device is introduced. The commercial software CFD-ACE+^{TM} is utilized to investigate the influences of various flow rates of the system on the temperature uniformity of the chip. The present paper also conducts some thermal measurements and PCR experimental works in order to complete the contents of this article.

Design concept

With the integration of one heater onto the chip center and two heat pipes on the opposite sides of the chip, constructing five temperature regions within a small chip for PCR can be achieved in our study. This can greatly reduce the chip size and the thermal control cost. By enlarging the channel width at the extension region, the residence time during the extension stage can be prolonged due to the decreased flow rate. The fluid properties in our simulations are thermal diffusivity, α, of 1.39×10^{-7} m^2/s, kinematic viscosity, ν, of 1×10^{-6} m^2/s, and density, ρ, of 1×10^3 kg/m^3. Five temperature regions are located within the chip width of 25 mm. The three temperature regions at the central part (6 mm wide) and the opposite sides of the chip (6 mm wide) supported by one heater and two heat pipes are at temperatures of 368 K and 328 K respectively. The inlet thermal boundary condition of the microchannel is set at 300 K. The above values of the parameters are used unless noted otherwise.

Numerical simulations are conducted on the heat and mass transfer for the present PCR device incorporating heating and cooling modules in order to ensure stable and accurate heat transfer from the heating plate to the PCR mixtures. In order to perform a comprehensive analysis of the fluid flow and heat transfer mechanism in the chip, the cross-sectional temperature distributions are utilized to demonstrate the flow and thermal characteristics inside the chip. The influences of various sample flow rates on the cross-sectional temperature distributions at half the channel height above the interface of the glass and PDMS bonding chip (AA cross

section) are, respectively, illustrated in Figs. 4(a)–4(f). The temperature distribution at the AA cross section can be treated as the temperature of the PCR mixture flowing along the microchannel. Flow rates of 0.2, 0.5, 1, 5, 10, and 50 μl/min are considered; these flow rates correspond to inlet flow velocities of 0.44, 1.11, 2.22, 11.11, 22.22, and 111.11 mm/s, respectively, and Re of 0.039, 0.097, 0.195, 0.975, 1.949, and 9.747, respectively. The flow in the microchannel can be considered to be laminar. From Fig. 4(a), the thermal carpet plot shows the three distinct and uniform temperature regions in the center area (for denaturation) and at the two sides of the chip (for annealing). Each extension region can be created by lateral heat conduction from the denaturation region to the annealing region (the area located at the enlarged part of the channel). How to construct five-temperature regions within a chip for PCR is apparent. The area with the lowest temperature is near the channel inlet. The influence of the inlet temperature on the temperature uniformity is negligible owing to the low sample flow rate. For a laminar flow with a small Re, the fluid will reach the equilibrium temperature very quickly. The heat convective effect inside the microchannel is related to the chip material, the flow velocity and the fluid properties[19] and can be neglected along the microchannel. The sample temperature is a little lower than that of the chip body as shown in Fig. 4(a). By increasing the

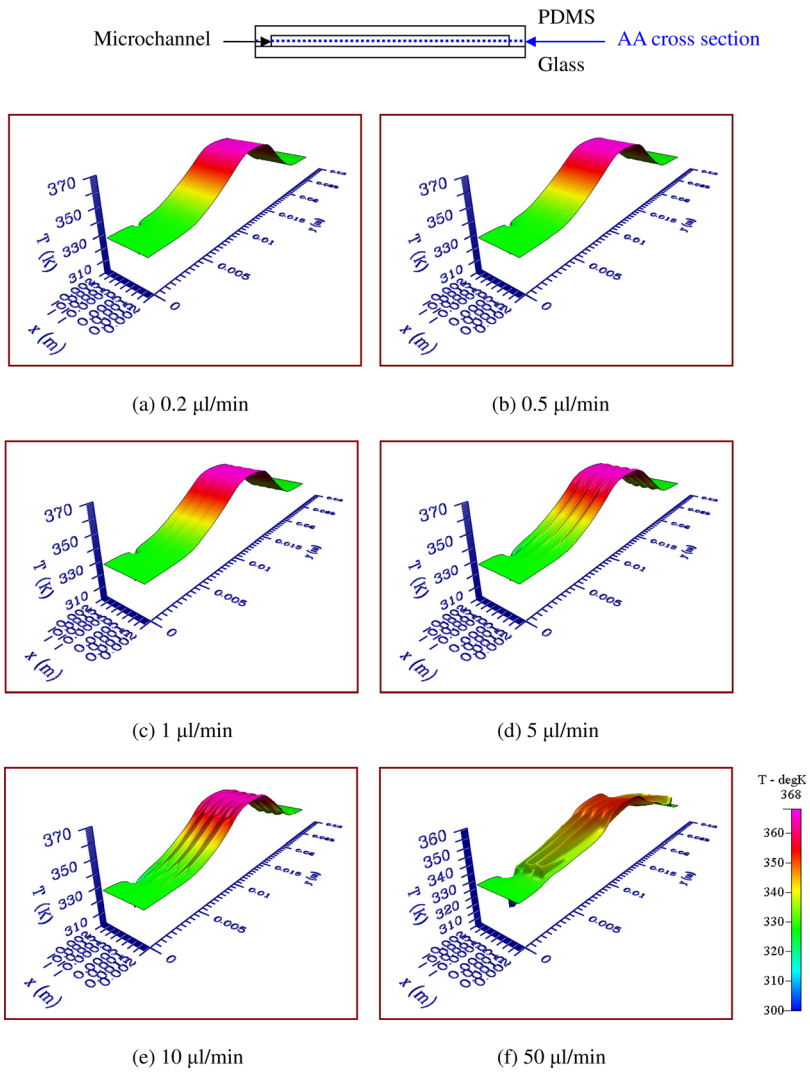

FIG. 4. The influences of various sample flow rates on the cross-sectional temperature distributions at half the channel height above the interface of the glass and PDMS bonding chip (AA cross section). Flow rate of (a) 0.2, (b) 0.5, (c) 1, (d) 5, (e) 10, and (f) 50 μl/min is considered

flow velocity, the heat convective effect inside the channel is enhanced and the temperature of the solid channel is also greatly influenced by the fluid flow. Results reveal that the temperature differences between the channel and the solid regions near the channel are increased more as the sample flow rates become larger as shown from Figs. 4(a)–4(f). In Fig. 4(f), when the flow rate is increased to 50 μl/min, the influence of the inlet temperature on the chip temperature is obvious. We find that the maximum temperature at the cross section is lower than 360 K so the predicted temperature distributions are not suitable for PCR.

The simulated results of the temperature profile along the central line of the denaturation region on the AA cross section (blue solid arrow) are expressed in Fig. 5. The required temperature at the denaturation region is set to be 368 K, and the purple dashed line in Fig. 5 represents the temperature 366 K. Along any temperature profile, the region near the local maximum is the solid region of the chip, and the region near the local minimum is the liquid region of the chip. The maximum temperature difference between the flow liquid and the solid regions near the channel at the denaturation region, ΔT_{max}, is less than 2 K when the flow rate is less than 5 μl/min. So, the effect on the temperature distribution due to convective heat transfer inside the microchannel is assumed to be negligible when the flow rate of the sample in the microchannel is less than 5 μl/min. Because of the information found in prior literature,[2,5,8,12,14,15,26–31] in order to make sure that the DNA amplification process is successful, the Re of the sample flow inside the microchannel was chosen to be less than 1. In our simulated results, the uniformity of the chip temperature at a specific reaction region is assured when the flow rate of the sample in the microchannel is less than 5 μl/min or the Re of the sample flow is less than 1. Our simulated results agree with the previous works. ΔT_{max} for the flow rate between 5 and 10 μl/min is also smaller than 2 K. However, due to the high convective effect, the temperature near the denaturation region is lower than 365 K. A denaturation temperature that is too low may cause either diffuse smearing upon gel electrophoresis or poor DNA amplification efficiency. This temperature distribution inside the flow-through device is not recommended to perform PCR. ΔT_{max} for the flow rates of 30 and 50 μl/min is larger than 9 and 13 K, respectively (demonstrated by the blue oval in Fig. 5). Results indicate that the chip temperature near the inlet is apparently lower than that away from the inlet due to the strong heat convection. Furthermore, the temperature of the denaturation region is less than 360 K, and the temperature distributions in the flow-through PCR device do not fit with the requisite PCR temperatures.

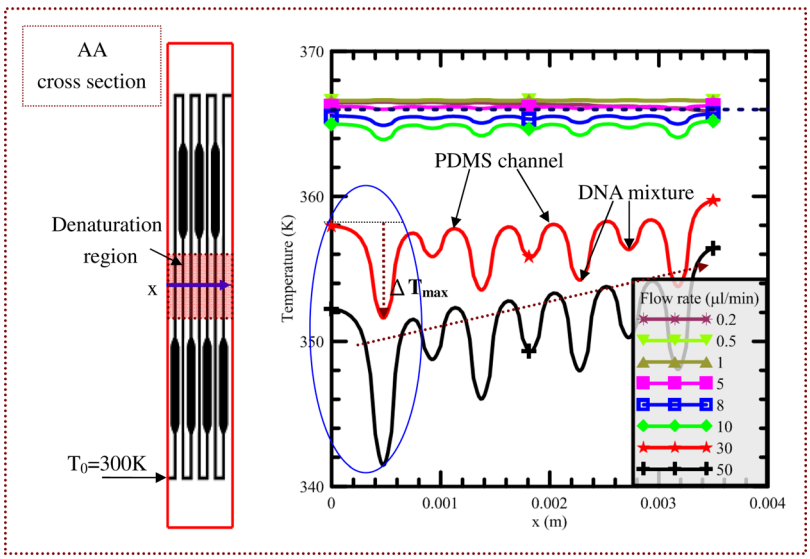

FIG. 5. The simulated results of the temperature profile along the central line of the denaturation region on the AA cross section (blue solid arrow).

The sample flow rate strongly affects the temperature distribution of the microfluidic chip and also has a straight impact on the residence time. In Fig. 6(a), the schematic diagram of the channel pattern with five reaction regions is shown (not in scale). The influences of various flow rates on the temperature profile along the pathline shown in Fig. 6(a) from point A to point B are presented in Fig. 6(b). A pathline is the trajectory that individual fluid particles follow. This can be thought of as tracing the path of a fluid element in the flow over a certain period. The temperature profile along the pathline is considered to be the sample temperature when the sample flows through the microchannel. Results show that the temperature profile for each cycle is almost identical when the sample rate is less than 5 μl/min, and the thermal cycling temperature profiles are clearly demonstrated. When the flow rate is less than 5 μl/min, the reaction temperatures for PCR are achieved and maintained for a significant proportion of the thermal cycle during the denaturation (high temperature) and annealing (low temperature) regions. Increasing the flow rate to 10 μl/min raises the forced convection effect of the fluid and this has a significant influence on the temperature field in the channel. The sample temperature of the denaturation region is 2 K lower than the requested denaturation temperature and the

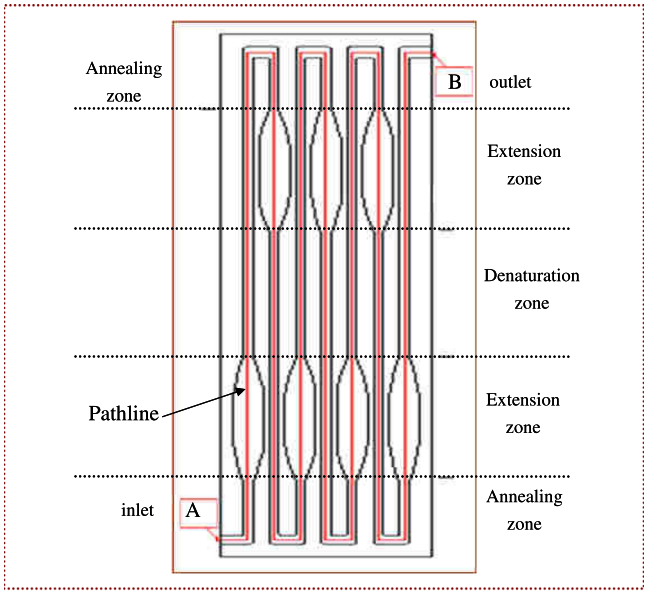

(a)

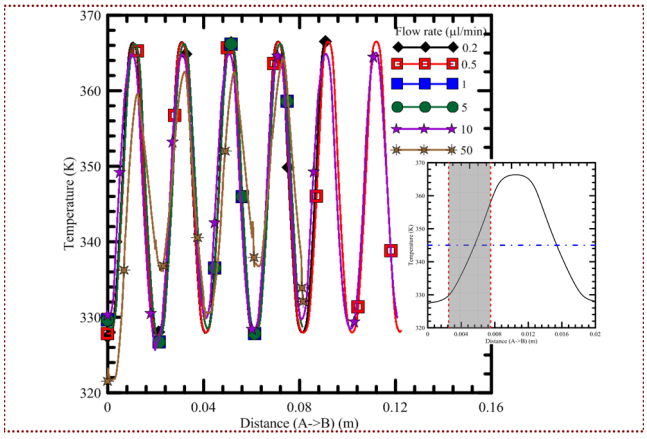

(b)

FIG. 6. (a) The schematic diagram of the channel pattern with five reaction regions is shown (not in scale). (b) The influences of various flow rates on the temperature profile along the pathline from point A to point B.

annealing region is 2 K higher than the requested annealing temperature. The desired temperatures can be readily achieved when the fluid moves at a flow rate of less than 5 μl/min. However, when the fluid flows at a speed greater than 10 μl/min, a lot of thermal energy from the heater will be carried by the moving fluid, and the rising time for the sample to reach the requested temperature is longer than the residence time. Thus, the differences between the sample temperature and the requested reaction temperature become greater with the increasing of the sample flow rate. The grey area enclosed by two vertical dashed lines is the location of the extension region that has the largest temperature gradients. The reaction temperature for the extension stage is set to be 345 K and described by the blue dotted-dashed line. The result shows that the requested extension region with the enlarged channel width can be obtained. At the flow rate of 2 μl/min, the average velocity of the sample fluid along the channel with a width of 150 μm is 2.723 mm/s, and the average velocity in the channel with a width of 540 μm is 0.641 mm/s. Because the residence time is proportional to the inverse of the average velocity, the residence time at the extension region with an enlarged channel width is 4.25 times longer than that without an enlarged channel width. Similar results are also obtained for the sample flow rate of less than 50 μl/min. Thus, by the rearrangement and enlargement of the channel width at the extension region, the residence time during the extension stage can be properly extended.

In the flow-through PCR chip, uniform temperature regions create the working regions. Large working regions are necessary to allow enough time for temperature cycling. The simulated results of the temperature distributions for the cross sections of the whole chip are shown in Fig. 7. In our experimental work, the sample flow rate is selected to be lower than 5 μl/min to complete the PCR process. So, the thermal convection effect along the microchannel on the chip temperature is negligible and the temperature of the sample flow is almost equal to that near the solid wall of the chip. In the following, the volume of the microchannel is not included in the simulation. As the thermal conductivity of the material for the PDMS-glass bonding chip is larger than that of the other polymer materials (e.g., polycarbonate, PMMA, etc.) used in microfluidic chips, the non-uniformity of the temperature distribution for the PDMS-glass bonding chip is small.[2] Results shown in Figs. 7(a) and 7(b) demonstrate the cross-sectional temperatures at the interface of the PDMS-glass bonding chip (cross section (a)) and the surface of the PDMS substrate (cross section (b)), respectively. We find that the temperature is very uniform along the x-direction. Only the temperature at the outer region of the cross-sectional area is a little lower than the temperature at the inner region. Part of the thermal energy from the heater is transferred into the interior region of the chip. The rest of the thermal energy transferred from the heater is stored near the outer region of the chip and then dissipated by air convection to the surrounding area. The temperature distribution shown in Fig. 7(a) can be treated as the temperature of the PCR mixture flowing along the microchannel. For a PDMS-glass bonding chip, the thermal conductivity of PDMS is about one-fifth the thermal conductivity of glass. Heat transfer occurs less efficiently across the upper PDMS substrate, which enlarges the temperature variation along the z-direction. The temperature difference of the PDMS-glass bonding chip between cross section (a) and cross section (b) can be observed by comparing Figs. 7(a) and 7(b). Figure 7(c) also illustrates the up-view pattern for the chip, and four cross-sectional locations of the chip from the boundary of the PDMS substrate at $s = 0.1$ mm, 3.5 mm, 8.8 mm, and 17.5 mm are also noted with (d), (e), (f) and (g), respectively. The working region of the sample DNA during PCR is from $s = 8.0$ mm to 28.7 mm (grey region). The cross-sectional temperature distributions at 4 locations−(d), (e), (f), and (g) shown in Fig. 7(c)−are demonstrated from Figs. 7(d) to 7(g). The difference between the adjacent contour lines is 4 K. The contour lines at the glass substrate are almost vertical to the bottom of the glass substrate, which confirms the slight temperature gradient along the z-axis. The temperature near the boundary of the PDMS substrate shown in Fig. 7(d) is slightly lower than that in Fig. 7(e). The temperature distributions from Figs. 7(e) to 7(g) are almost the same. This indicates that the temperature uniformity at the region from $s = 3.5$ mm to 31.5 mm is unambiguous, and this region covers the whole PCR working region. The denaturation region with a temperature of about 367 K and the annealing region with a temperature of about 328 K are found at

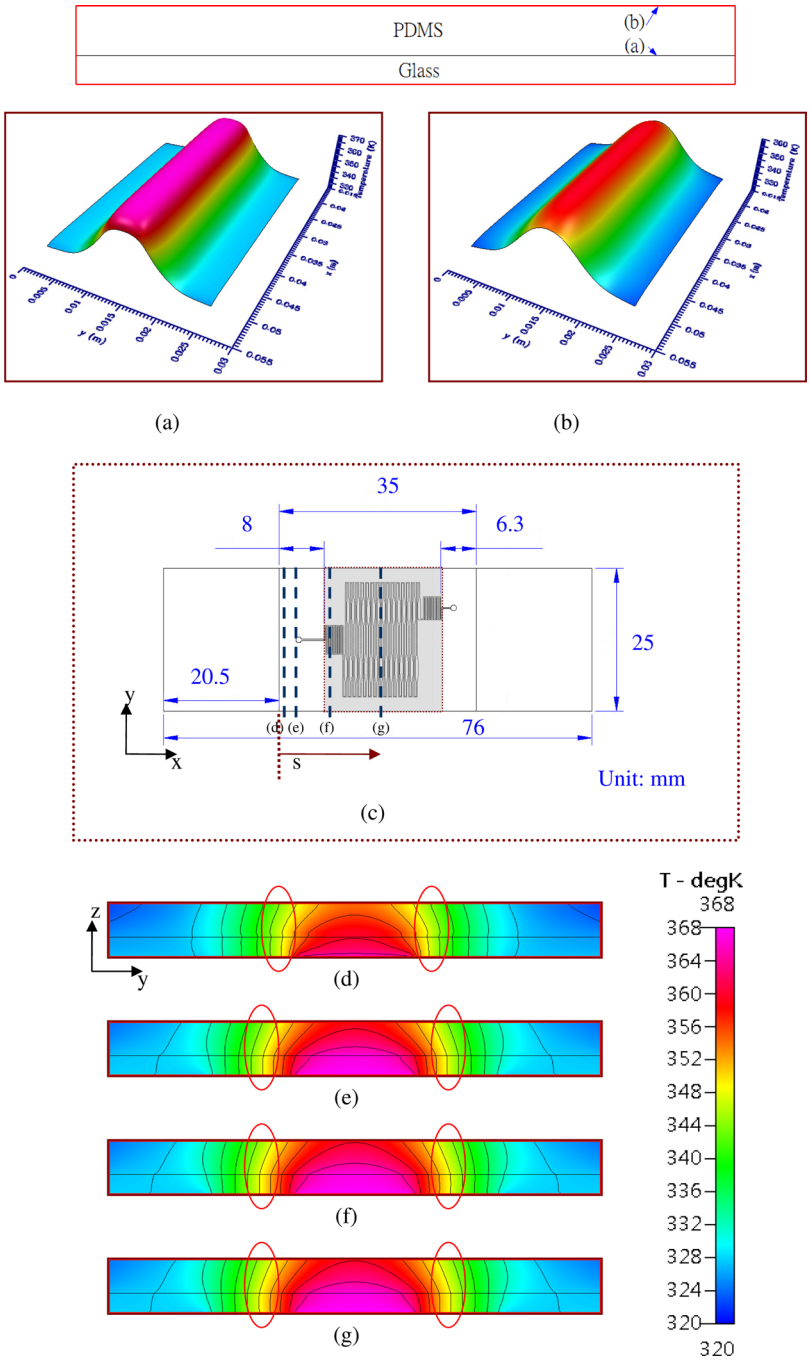

FIG. 7. The simulated results of the temperature distributions for the cross sections of the whole chip. The cross-sectional temperatures at (a) the interface of the PDMS-glass bonding chip (cross section (a)) and (b) the surface of the PDMS substrate (cross section (b)). (c) The up-view pattern for the chip, and four cross-sectional locations of the chip from the boundary of the PDMS substrate at s = 0.1 mm, 3.5 mm, 8.8 mm, and 17.5 mm. The cross-sectional temperature distributions at 4 locations—(d), (e), (f), and (g).

the interface of the chip at the central part and at the opposite sides of the chip. In addition, the extension region of about 345 K also exists between the denaturation and annealing region of the chip (marked by a red circle).

A five-temperature-region PCR chip is obtained in our study. The temperature differences between the chip surface and the PCR mixture at the denaturation, annealing, and extension regions are about 7.1 K, 3.8 K, and 3.5 K, respectively. During the PCR experiments, the

measured surface temperatures are usually utilized to make sure that the chip setting temperatures are reached. The required PCR temperatures can be obtained by measuring the surface temperature of the chip and then adding the temperature difference between the chip surface and the PCR mixture. The accuracy of the required PCR temperatures is dependent on the locations of the measured points. Thus, in our designed device, any measured point on the PDMS upper surface at the working region can be used to achieve the required PCR temperatures without doubt.

Validation of thermal arrangement by heat pipes

In order to enhance the flexibility of the one-heater PCR chip, heat pipes with high thermal conductance and low expenditure are utilized in our study to create the annealing temperature regions of the chip. Thus, constructing five temperature regions within a small chip for PCR is obtained. No comprehensive numerical calculations and repetitive experiments for the chip geometry and the heater arrangement are needed before the fabrication of the device.

To validate the thermal arrangement of two heat pipes under the opposite sides of the flow-through PCR device, three methods for measuring chip temperatures are employed in our study. The surface temperatures of the chip with the sample flow rate of 2 μl/min are measured by infrared imager. Ten paths are defined across the chip as shown in Fig. 8(a). The temperatures at thirty points for each path are recorded. The average temperatures of these paths are calculated from the experimental results. The channel temperatures are measured using thermocouples which are injected into slots. Four electric wires are patterned and used to be the mold of the slots for injecting the thermocouples, shown in the left hand side of Fig. 8(b). The PDMS mixture is then cast into the mold. This molding method is similar to the traditional PDMS molding method. The bonding chip for measuring temperatures is assembled and demonstrated in the right hand side of Fig. 8(b). The marked points on the

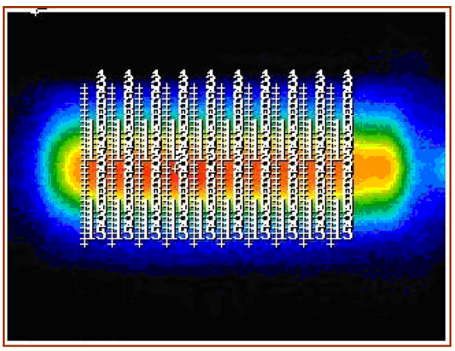

(a)

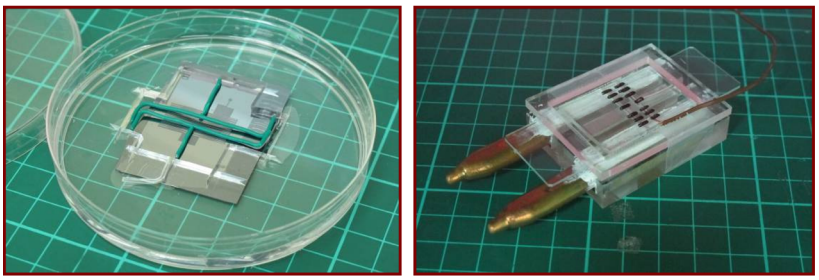

(b)

FIG. 8. (a) The surface temperatures of the chip with the sample flow rate of 2 μl/min measured by infrared imager. Ten paths are defined across the chip. (b) Four electric wires are patterned and used to be the mold of the slots for injecting the thermocouples. The bonding chip for measuring temperatures is assembled and demonstrated.

PDMS substrate are the locations of the measuring points. Some thermocouples are inserted into the PDMS-based chip and contacted with the glass to monitor the temperatures. The surface temperatures of the chip with various fan powers for cooling the heat pipes are measured by the infrared imager and the thermocouples. The influences of various cooling conditions on the average temperature profiles are illustrated in Fig. 9. The solid lines with marked symbols indicate the temperatures measured by the infrared imager, and the marked symbols without the lines represent the temperatures measured by the thermocouples. Results confirm the clear temperature differences on the chip surface resulting from different fan powers. When using a fan with an input voltage of 5 V, the lowest temperature at the annealing region can reach 5.93 K less than that with 0 V. Furthermore, with the input voltage increasing to higher than 8 V, the lowest temperature at the annealing region can be decreased to 13.17 K less than that with 0 V. The effect of forced convection cooling is very clear. Similar results can be seen for the measured temperatures from the thermocouples in Fig. 9. Due to the high thermal conductivity of glass, the measured temperatures are almost the same as the heater temperatures. Some thermocouples which are inserted into the slots of the bonded chip are utilized to measure the temperatures at several specified points. We find that the temperature difference between the chip surface (measured by the IR imager) and the PCR mixture (measured by the thermocouples) is about 10.6 K. Because of the contact resistance between the chip and the heat pipes, the contact resistance between the chip and the heater, the tentative locations of the thermocouples, and the uncertain natural convection heat transfer coefficient from the device to the ambient, some discrepancies exist between the temperatures by numerical simulation and by measurement.

The effect of the fluid transport on the temperature distribution can be visualized qualitatively using a thermally sensitive dye. Using the thermally sensitive dye with an approximate transition temperature of 343 K, the visualization of the channel temperature distribution can be observed. The dye becomes colorless when the temperature is greater than approximately 343 K and darker when the temperature is lower than roughly 343 K. Figure 10(a) clearly shows that the transition point lies between the heating block and the heat pipes when the fluid with dye is moving at the flow rate of 2 μl/min. The numerical temperature distribution shown in Fig. 10(b) is almost the same as the experimental result. In our study, the extension temperature is set to be 345 K and is near the transition temperature of the dye. We find that the transition region

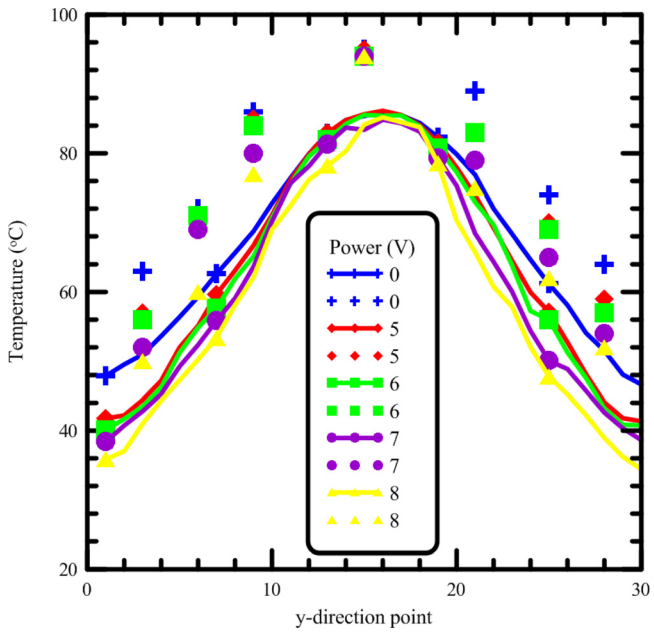

FIG. 9. The influences of various cooling conditions on the average temperature profiles.

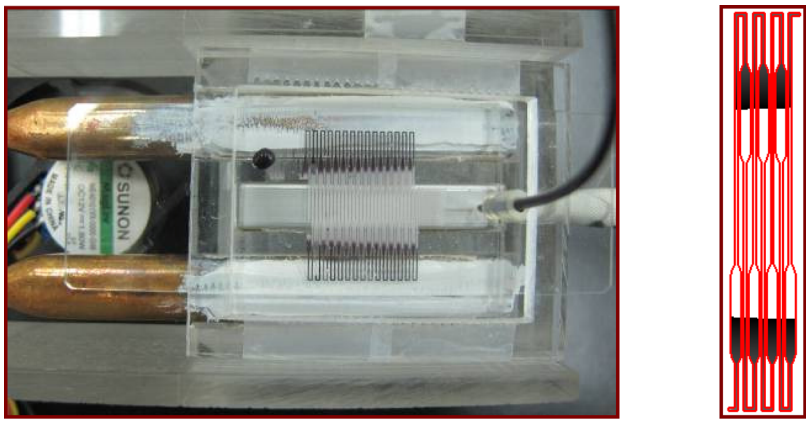

(a) (b)

FIG. 10. (a) The effect of the fluid transport on the temperature distribution visualized qualitatively using a thermally sensitive dye. The transition point lies between the heating block and the heat pipes when the fluid with dye is moving at the flow rate at 2 μl/min. (b) The numerical temperature distribution.

for the thermally sensitive dye is located at the enlarged channel. Thus, the requested extension region with an enlarged channel width can be realized.

PCR experiments

Surface adsorption of proteins (i.e., *Taq* polymerase) is a critical issue regarding micro PCR devices. With the high surface to volume ratios of flow-through PCR microdevices, polymerase adsorption is one of the major causes of amplification failure. This PCR inhibition may be due to polymer-protein interaction, which might prevent polymerase from moving onto the DNA chain, and therefore inhibit PCR. PDMS is a commonly used material for microfluidic devices, and the hydrophobicity of the PDMS surface causes strong adsorption of proteins. As a possible solution to this problem, plasma treatment is examined, which is applied to create an irreversible bond between PDMS and glass. This treatment causes the surface to become hydrophilic (contact angle is less than 90°), thus reducing the interaction between the proteins and the surface. However, the initial hydrophobic effect reappears a period of time later so this solution does not seem to be a practical approach.[32]

Static and dynamic passivation techniques are frequently applied in PCR microfluidics in order to modify the microchannel inner surface to be hydrophilic so as to decrease the adsorption of the proteins onto the inner surface. The PDMS channel is filled with the passivation solution and kept still for an interval. This treatment is the static surface modification. The addition of the passivation solution into the PCR mixture is the dynamic surface modification method. Using both surface modification methods prevents protein absorption more efficiently. In our study, only the static passivation method is utilized. The PDMS substrates that have been individually immersed into the passivation solutions are utilized and the contact angles are measured. A 2 mm thick PDMS substrate is cut into pieces of 15 mm × 15 mm, rinsed with copious amounts of deionized water, and blown dry with nitrogen. The substrates are then immersed into the solutions of 20% Tween 20 and BSA (1 mg/ml), respectively, at room temperature for 1 h and blown dry with nitrogen. Then, these surface-modified PDMS substrates are used for measuring the contact angles (FTA1000B Drop Shape Analysis System, First Ten Angstroms, Inc., USA).

Images from the drop shape analysis system are demonstrated in Fig. 11.They show the contact angles of a water drop on an untreated or treated PDMS surface at 2 days and two weeks. The mean values of the measurements at four measured times (i.e., 1 day, 2 days, one week, and two weeks) are used and also shown in Fig. 11. The contact angle of untreated

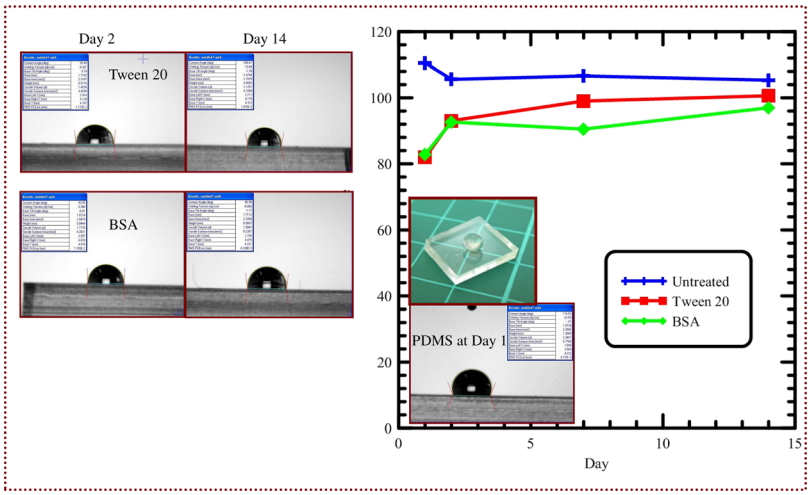

FIG. 11. Images from the drop shape analysis system, and the contact angles of a water drop on an untreated or treated PDMS surface at 2 days and two weeks. The mean values of the measurements at four measured times (i.e., 1 day, 2 days, one week, and two weeks).

PDMS substrates remains at around 105°–112° within two weeks. According to literature,[8] the contact angle of pure PDMS is greater than 105°. The results also demonstrate the contact angle changes on the PDMS surfaces with the surface modification solutions. Time-dependent change in contact angle occurs because of the release of surfactant to the ambient environment. The contact angle decreased to 81°, and 82°, after 1-day treating with Tween 20, and BSA, respectively. Within 2 days, the treated surfaces remain hydrophilic. After 2 weeks, the contact angle gradually returns to 100°, and 96° for treatments with Tween 20, and BSA, respectively.

Amplification of a 385-bp DNA fragment is carried out, respectively, on the flow-through PCR device as well as the commercial PCR machine. Due to the gradual recovery of surface hydrophobicity, the effect of surface treatments on PCR efficiency is evaluated immediately after the static passivation method. The surface of the microchannels is statically modified with Tween 20 (20%) and BSA (1 mg/ml) solution for 1 h in advance, respectively. After pushing out the solutions inside the microchannel, the channels are rinsed with double distilled water and the PCR reaction mixture is then injected into the channel. The PCR product is collected into a tube after the amplification is completed. Fig. 12 illustrates the results of gel electrophoresis analysis of the products. The first lane (Lane 1) indicates the DNA ladder. Results shown at the top of Fig. 12 clearly present the 385-bp PCR product in the commercial PCR machine (Lane 2), Tween 20 (Lanes 3 and 5), and BSA (Lanes 4 and 6). Coating the PDMS substrate with the surfactant molecules demonstrates fairly efficient protein resistance. The results from the flow-through PCR device are comparable to those obtained by the commercial PCR machine. Therefore, the present device provides a low-cost alternative PCR system for the amplification and analysis of target DNA fragments. Images are analyzed using image processing software (ImageJ, version 1.48, NIH, USA). Intensity linescans of the fluorescence intensities are utilized to determine those intensities. The bottom of Fig. 12 also illustrates the grey intensities of PCR products by image analysis. Although slightly weaker PCR band intensities of Lanes 3 to 6 than those of Lane 2 are observed, they are sufficient for evaluations and analyses in diagnoses. The static treatment of the microchannel by BSA[8,33] and Tween 20[2,34] was proved to be a useful approach to reduce the protein adsorption in previous studies and also presents an efficient amplification of DNA segments in our chip device.

From Fig. 12, it can be seen that the result of protein adsorption is a very poor PCR reaction due to the hydrophobicity of the untreated PDMS substrate. The static passivation method with Tween 20 (20%) or BSA (1 mg/ml) solution is utilized to increase the hydrophilicity of

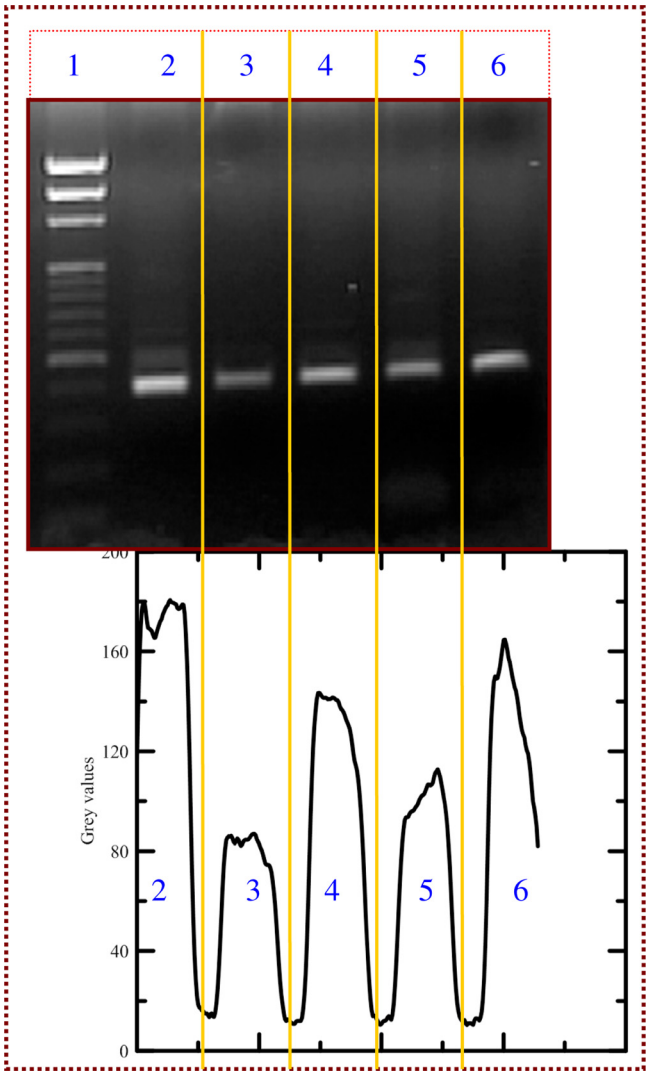

FIG. 12. The results of gel electrophoresis analysis of the products. The first lane (Lane 1) indicates the DNA ladder. The 385-bp PCR product in the commercial PCR machine (Lane 2), Tween 20 (Lanes 3 and 5), and BSA (Lanes 4 and 6). And the grey intensities of PCR products by image analysis.

the channel surface and decrease the adsorption of the proteins onto PDMS surfaces. This method proved to present efficient amplifications of DNA segments in our chip device.

CONCLUSIONS

To our knowledge, our group is the first group to use the heat pipe cooling module that has been applied to the design of a PCR device. By utilizing the heating module to support the denaturation region and the cooling module to obtain the annealing region, the extension region can be created by lateral heat conduction from the denaturation region to the annealing region. Numerical simulations and thermal measurements have shown that the temperature distribution in the five-temperature-region PCR chip can be suitable for DNA amplification. Furthermore, by the rearrangement and enlargement of the channel width at the extension region, the residence time during the extension stage can be properly extended. So, this system can reduce the reaction time and the space of the serpentine-channel PCR chip and also greatly reduce the thermal control cost. In the simulated results, the maximum temperature difference between the flow liquid and the solid regions near the channel at the denaturation region, ΔT_{max}, is less than

2 K when the flow rate is less than 5 μl/min. The uniformity of the chip temperature at each specific reaction region is assured, and the reaction temperatures for thermal cycling are achieved and maintained for a significant proportion of the thermal cycle during the denaturation (high temperature) and annealing (low temperature) regions when the Re of the sample flow is less than 1. Also indicated is that the temperature uniformity at the region from s = 3.5 mm to 31.5 mm is unambiguous, and the region covers the whole PCR working region. Thus, any measured point at the working region of the sample DNA can be used to achieve the required PCR temperatures without doubt. The treated surfaces of the flow-through microchannel are characterized using the water contact angle; the effects of the hydrophilicity of the treated PDMS microchannels on PCR efficiency are determined by using gel electrophoresis. Increasing the hydrophilicity of the channel surface by immersing the PDMS substrates into Tween 20 (20%) or BSA (1 mg/ml) solution proved to present efficient amplifications of DNA segments in our chip device. The fabricated flow-through microreactor is successfully capable of DNA amplification and well applied to a low-cost PCR system.

ACKNOWLEDGMENTS

The authors thank the National Science Council of the Republic of China for financially supporting this research under Contract No. MOST 103-2313-B-020-006 -. Daryl Switak is appreciated for his editorial assistance.

[1]D. Liu, G. Liang, X. Lei, B. Chen, W. Wang, and X. Zhou, Anal. Chim. Acta **718**, 58 (2012).
[2]J. J. Chen, C. M. Shen, and Y. W. Ko, Biomed. Microdevices **15**, 261 (2013).
[3]C. T. Wittwer and D. J. Garling, Biotechniques **10**, 76 (1991).
[4]C. T. Wittwer, M. G. Herrmann, C. N. Gundry, and K. S. Elenitoba-Johnson, Methods **25**, 430 (2001).
[5]K. Sun, A. Yamaguchi, Y. Ishida, S. Matsuo, and H. Misawa, Sens. Actuators, B **84**, 283 (2002).
[6]M. Hashimoto, P. C. Chen, M. W. Mitchell, D. E. Nikitopoulos, S. A. Soper, and M. C. Murphy, Lab Chip **4**, 638 (2004).
[7]S. Mohr, Y. H. Zhang, A. Macaskill, P. J. R. Day, R. W. Barber, N. J. Goddard, D. R. Emerson, and P. R. Fielden, Microfluid. Nanofluid. **3**, 611 (2007).
[8]I. Kuan, W. Gu, J. Wu, C. Wei, K. Chen, and C. Yu, Chem. Eng. J. **143**, 326 (2008).
[9]T. Nakayama, H. M. Hiep, S. Furui, Y. Yonezawa, M. Saito, Y. Takamura, and E. Tamiya, Anal. Bioanal. Chem. **396**, 457 (2010).
[10]Q. Cao, M. Mahalanabis, J. Chang, B. Carey, C. Hsieh, A. Stanley, C. A. Odell, P. Mitchell, J. Feldman, N. R. Pollock, and C. M. Klapperich, PLoS One **7**, e33176 (2012).
[11]N. Crews, C. Wittwer, and B. Gale, Proc. SPIE **6465**, 646504-1 (2007).
[12]W. Wu and N. Y. Lee, Anal. Bioanal. Chem. **400**, 2053 (2011).
[13]A. G. Sciancalepore, E. Mele, V. Arcadio, F. Reddavide, F. Grieco, G. Spano, P. Lucas, G. Mita, and D. Pisignano, Food Microbiol. **35**, 10 (2013).
[14]K. T. L. Trinh, W. Wu, and N. Y. Lee, Sens. Actuators B **190**, 177 (2014).
[15]S. Li, D. Y. Fozdar, M. F. Ali, H. Li, D. Shao, D. M. Vykoukal, J. Vykoukal, P. N. Floriano, M. Olsen, J. T. McDevitt, P. R. C. Gascoyne, and S. Chen, J. Microelectromech. Syst. **15**, 223 (2006).
[16]M. Hashimoto, F. Barany, and S. A. Soper, Biosens. Bioelectron. **21**, 1915 (2006).
[17]A. Reichert, J. Felbel, M. Kielpinski, M. Urban, B. Steinbrecht, and T. Henkel, J. Bionic. Eng. **5**, 291 (2008).
[18]S. Thomas, R. L. Orozco, and T. Ameel, Microfluid. Nanofluid. **17**, 1039 (2014).
[19]J. P. Holman, *Heat Transfer*, 10th ed. (McGraw-Hill, New York, 2009).
[20]J. P. van Doormaal and G. D. Raithby, Numer. Heat Transfer **7**, 147 (1984).
[21]T. J. Barth and D. C. Jespersen, in 27th Aerospace Sciences Meeting and Exhibit, Reno, Nevada, USA, AIAA-89-0366 (1989).
[22]R. Wienands and W. Joppich, *Practical Fourier Analysis for Multigrid Methods* (Chapman and Hall/CRC, Virginia Beach, 2005).
[23]P. Sonneveld, SIAM J. Sci. Stat. Comp. **10**, 36 (1989).
[24]J. A. Kim, J. Y. Lee, S. Seong, S. H. Cha, S. H. Lee, J. J. Kim, and T. H. Park, Biochem. Eng. J. **29**, 91 (2006).
[25]A. Polini, E. Mele, A. G. Sciancalepore, S. Girardo, A. Biasco, A. Camposeo, and D. Pisignano, Biomicrofluidics **4**, 036502 (2010).
[26]M. U. Kopp, A. J. De Mello, and A. Manz, Science **280**, 1046 (1998).
[27]I. Schneegaß, R. Bräutigam, and J. M. Köhler, Lab Chip **1**, 42 (2001).
[28]P. J. Obeid and T. K. Christopoulos, Anal. Chim. Acta **494**, 1 (2003).
[29]S. R. Joung, C. J. Kang, and Y. S. Kim, Jpn. J. Appl. Phys., Part 1 **47**, 1342 (2008).
[30]T. H. Fang, N. Ramalingam, D. Xian-Dui, T. S. Ngin, Z. Xianting, A. T. Lai Kuan, E. Y. Peng Huat, and G. Hai-Qing, Biosens. Bioelectron. **24**, 2131 (2009).
[31]D. Y. Kong, T. W. Kang, C. T. Seo, C. S. Cho, and J. H. Lee, BioChip J. **4**, 179 (2010).
[32]J. J. Chen, S. C. Liao, M. H. Liu, J. D. Lin, T. S. Sheu, and J. M. Miao, Micromachines **5**, 116 (2014).
[33]Z. R. Xu, X. Wang, X. F. Fan, and J. H. Wang, Microchim. Acta **168**, 71 (2010).
[34]P. C. Chen, W. Fan, T. K. Hoo, L. C. Z. Chan, and Z. Wang, Chem. Eng. Res. Des. **90**, 591 (2012).